

# TCAD-Oriented Physical Modeling of Temperature-Dependent Inversion Layer Mobility in SiC MOSFETs

Tetsuo Hatakeyama

*Dept. of Electrical and Electronic Engineering (EEE)  
Toyama Prefectural University (TPU)  
Imizu, Toyama, Japan  
0000-0003-2277-048X*

Hirohisa Hirai

*Advanced Power Electronics Research Center (ADPERC)  
National Institute of Advanced Industrial Technology (AIST)  
Tsukuba, Ibaraki, Japan  
0000-0002-2802-2282*

Mitsuru Sometani

*ADPERC  
AIST*

*Tsukuba, Ibaraki, Japan  
0000-0002-8208-8469*

Dai Okamoto

*Dept. of EEE  
TPU*

*Imizu, Toyama, Japan  
0000-0003-2494-1764*

Mitsuo Okamoto

*ADPERC  
AIST*

*Tsukuba, Ibaraki, Japan  
0000-0003-3261-8705*

Shinsuke Harada

*ADPERC  
AIST*

*Tsukuba, Ibaraki, Japan  
0000-0002-0053-4606*

**Abstract**—Closed-form mobility models for SiC MOS interfaces were developed based on scattering theory, explicitly incorporating temperature dependence using power-law approximations. These models improve the physical accuracy and predictive capability of TCAD simulations for SiC MOSFETs, and provide insight into the dominant scattering mechanisms at the interface.

**Index Terms**—Silicon Carbide, MOSFET, Inversion layer, mobility, Modeling, dipole scattering, Coulomb scattering

## I. INTRODUCTION

Silicon carbide (SiC) MOSFETs are widely recognized as promising power devices owing to their superior properties, such as high breakdown voltage, high-temperature operation, and low switching loss. In low-voltage-rated ( $\leq 1200$  V) SiC MOSFETs, the channel resistance ( $R_{ch}$ ) constitutes a major portion of the total on-resistance ( $R_{on}$ ) and thus plays a critical role in device performance. Accurate prediction of  $R_{ch}$  is therefore essential for device design and requires a mobility model that captures the physical characteristics of the inversion layer at the SiC/SiO<sub>2</sub> interface.

The inversion layer mobility is influenced by electric field, carrier density, and temperature. To enable reliable TCAD-based device simulation, it is vital to develop a physically based model that not only improves the accuracy of performance prediction, but also provides insight into mobility-limiting mechanisms—thereby guiding device optimization. However, existing models face two major limitations when applied to SiC MOS interfaces:

- **Neglect of dipole scattering:** Unlike conventional Si MOSFETs, the inversion layer mobility in SiC MOSFETs

is significantly limited by dipole scattering [3], [4], which is believed to originate from microscopic dipoles associated with the conduction-band wavefunction in 4H-SiC, spontaneous polarization, or interfacial charge redistribution [2]. The exact physical origin remains unclear.

- **Lack of physical interpretation:** While empirical models exist for mobility as a function of temperature or electric field, they often lack a physical foundation, making their parameters difficult to interpret and limiting their usefulness for device design.

To address these issues, we propose a physics-based, closed-form mobility model that incorporates both dipole and Coulomb scattering mechanisms. The model is derived from the scattering theory of two-dimensional electron gases and explicitly includes temperature dependence. It enables accurate TCAD prediction of device performance, particularly under high-temperature conditions.

This work extends our earlier modeling efforts [3]–[5], incorporating key findings on interface traps and dominant scattering mechanisms at the SiC MOS interface. Here, we present the methodology and results for modeling the temperature dependence of inversion layer mobility in SiC MOSFETs.

## II. METHOD OF MODELING

To accurately reproduce the inversion layer mobility in SiC MOSFETs, it is essential to model both the interface states, which govern electron trapping, and the free carrier mobility itself. The impact of interface states was characterized using Hall effect measurements. For mobility modeling, our analysis based on scattering theory showed that dipole scattering is the dominant scattering mechanism at SiC MOS interfaces, as previously reported [4], [5].

This work was supported by the MEXT-Program for Creation of Innovative Core Technology for Power Electronics (Grant No. JPJ009777), JSPS KAKENHI Grant No. 23K03928, and the academic research grant from Toshiba Device & Storage Corporation.

We derived a closed-form expression for dipole scattering-limited mobility ( $\mu_{dp}$ ) by fitting the theoretical calculations with simple analytical functions. The mobility was expressed as a product of two separable functions: one depending only on the effective electric field ( $E_{eff}$ ), and the other on the sheet carrier density ( $n_s$ ):

The mobility was expressed as a product of functions of effective electric field ( $E_{eff}$ ) and sheet carrier density ( $n_s$ ):

$$\mu_{dp}(E_{eff}, n_s) = f(E_{eff}) \cdot g(n_s), \quad (1)$$

where

$$f(E_{eff}) = (E_{eff}/E_0)^{-\gamma}, \quad (2)$$

$$g(n_s) = \mu_0 \left(1 + \frac{n_s}{n_{s0}}\right) \left(\frac{n_{dp0} d_{dp0}}{n_{dp} d_{dp}}\right), \quad (3)$$

and the model parameters are listed in Table I. The effective electric field  $E_{eff}$  is defined as:

$$E_{eff} = \frac{q}{\epsilon_{SiC}} \left(N_{dpl} + \frac{11}{32} n_s\right), \quad (4)$$

where  $N_{dpl}$  is the areal density of the ionized acceptors in the depletion region.

TABLE I  
MODEL PARAMETERS FOR CLOSED-FORM EXPRESSION OF DIPOLE SCATTERING-LIMITED MOBILITY

Symbol	Value	Unit	Remarks
$\gamma$	0.9	1	exponent
$E_0$	1	MV/cm	normalization factor
$\mu_0$	148.19	cm <sup>2</sup> /V·s	
$n_{s0}$	$2.86 \times 10^{12}$	cm <sup>-2</sup>	
$n_{dp0}$	$1 \times 10^{13}$	cm <sup>-2</sup>	normalization factor
$d_{dp0}$	$1 \times 10^{-7}$	cm	normalization factor
$n_{dp}$	$3 \times 10^{13}$	cm <sup>-2</sup>	fitting parameter
$d_{dp}$	$1 \times 10^{-7}$	cm	fitting parameter
$T_0$	300	K	Room temperature
$\kappa$	1.2	1	exponent

To incorporate temperature dependence into the mobility model, we extend the  $n_s$ -dependent term  $g(n_s)$  to a temperature-dependent form  $g_t(n_s, T)$ , and introduce an additional factor  $h(T)$  to account for the remaining temperature effects. The resulting expression becomes:

$$\mu_{dp}(E_{eff}, n_s, T) = f(E_{eff}) \cdot g_t(n_s, T) \cdot h(T). \quad (5)$$

This formulation is based on the observation that the screening constant is proportional to  $n_s/T$ , which implies that part of the temperature dependence can be incorporated into  $g(n_s)$  by scaling with  $T$ . Assuming that the remaining temperature dependencies are separable from the field and density terms, we define  $g_t(n_s, T)$  as:

$$g_t(n_s, T) = \mu_0 \left(1 + \frac{n_s}{n_{s0}} \cdot \frac{T_0}{T}\right) \left(\frac{n_{dp0} d_{dp0}}{n_{dp} d_{dp}}\right). \quad (6)$$

To derive the functional form of  $h(T)$ , dipole scattering-limited mobility was calculated based on the scattering theory of a two-dimensional electron gas. The temperature dependence of the dipole scattering-limited mobility was evaluated

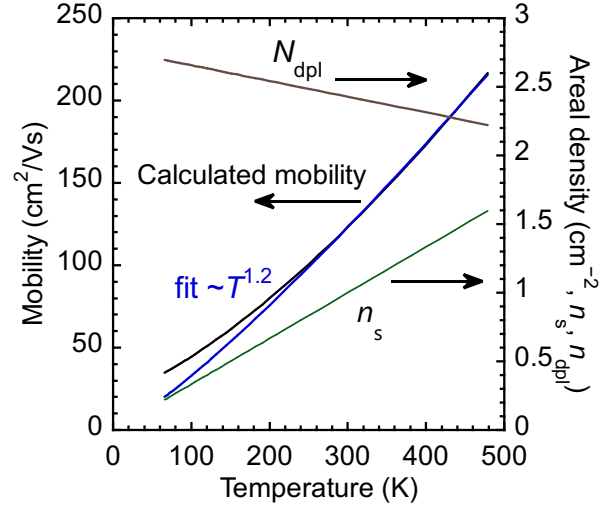


Fig. 1. Calculated mobility as a function of temperature under the conditions of constant effective electric field ( $E_{eff} = 0.5$  MV/cm) and constant screening effect ( $n_s/T = \text{const.}$ ). Also shown are the corresponding values of  $n_s$  and  $N_{dpl}$  adjusted at each temperature to maintain these conditions.

under the conditions of constant effective electric field and a fixed ratio of  $n_s/T$ .

Next, we describe the procedure used to determine the functional form of the temperature-dependent term  $h(T)$ . We begin by setting the initial sheet carrier density  $n_s$  at 300 K to  $1 \times 10^{12}$  cm<sup>-2</sup>. To maintain a constant screening effect, the ratio  $n_s/T$  is kept constant, and  $n_s$  is scaled proportionally with temperature during the calculation of mobility. Meanwhile, the effective electric field  $E_{eff}$  is kept constant. Since  $E_{eff}$  defined by Eq. 4 is a function of both  $n_s$  and  $N_{dpl}$ , the areal acceptor concentration is adjusted according to the variation in  $n_s$  to ensure that  $E_{eff}$  remains unchanged. This calculation setup is illustrated in Fig. 1, which shows the calculated temperature dependence of mobility under the conditions of constant effective electric field and constant screening effect. The corresponding temperature-dependent values of  $n_s$  and  $N_{dpl}$  used in the calculation are also plotted. The effective electric field is fixed at 0.5 MV/cm throughout this analysis.

Under these conditions, the mobility is evaluated with only temperature varied, while both the screening condition and  $E_{eff}$  are fixed. Accordingly, the field-dependent term  $f(E_{eff})$  and the density-dependent term  $g_t(n_s, T)$  remain constant, and the variation in mobility directly reflects the behavior of  $h(T)$ .

Physically, this configuration ensures that the shape of the carrier wavefunction—governed by  $E_{eff}$ —is unchanged, and that the screening condition characterized by  $n_s/T$  remains constant. In other words, the energy dependence of the momentum relaxation time is fixed, and the observed temperature dependence of mobility arises solely from the thermal averaging over the distribution function.

Through this procedure, we find that  $h(T)$  can be approximated by a power-law function of temperature, with an

exponent of approximately 1.2:

$$h(T) \propto T^{1.2}. \quad (7)$$

Figure 2 shows the calculated temperature dependence of dipole scattering-limited mobility for various effective electric fields, under the same screening conditions ( $n_s/T = \text{const.}$ ), which corresponds to  $n_s = 1 \times 10^{12} \text{ cm}^{-2}$  at 300 K. Figure 3 shows its temperature dependence for various screening conditions ( $n_s/T = \text{const.}$ ), with the effective electric field fixed at  $E_{\text{eff}} = 0.5 \text{ MV/cm}$ .

These results demonstrate that the temperature exponent  $\kappa \approx 1.2$  is consistently across a wide range of effective electric fields and screening conditions.

Based on these observations, the temperature dependence of mobility is approximated as:

$$h(T) = \left(\frac{T}{T_0}\right)^\kappa \quad \text{with} \quad \kappa = 1.2. \quad (8)$$

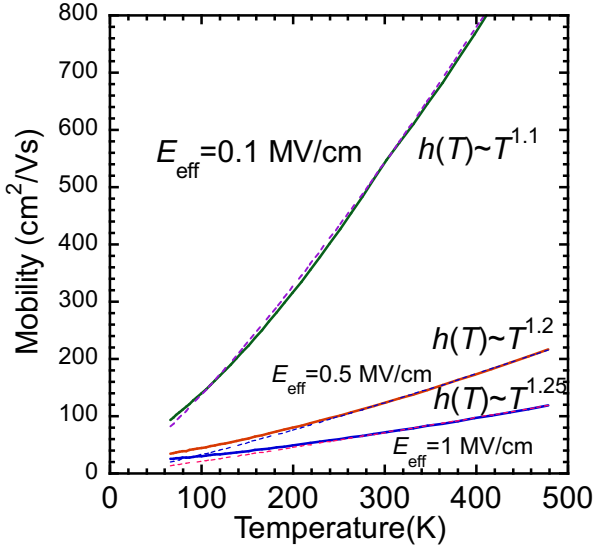


Fig. 2. Temperature dependence of dipole scattering-limited mobility under the constant screening condition ( $n_s/T = \text{const.}$ ), which corresponds to  $n_s = 1 \times 10^{12} \text{ cm}^{-2}$  at 300 K, for various effective electric fields  $E_{\text{eff}}$ .

The same approach used to incorporate temperature dependence into the closed-form expression for dipole scattering-limited mobility was also applied to Coulomb scattering-limited mobility. Specifically, the ratio  $n_s/T$  and the effective electric field  $E_{\text{eff}}$  were kept constant during the calculation, so that the influence of the carrier distribution function on the temperature dependence could be isolated and analyzed.

As a result, a closed-form expression for the Coulomb scattering-limited mobility was derived by assuming the same functional form as that used for the dipole case. The mobility is expressed as the product of functions that separately capture the dependencies on  $E_{\text{eff}}$ ,  $n_s$ , and temperature:

$$\mu_C(E_{\text{eff}}, n_s) = f(E_{\text{eff}}) \cdot g_t(n_s, T) \cdot h(T), \quad (9)$$

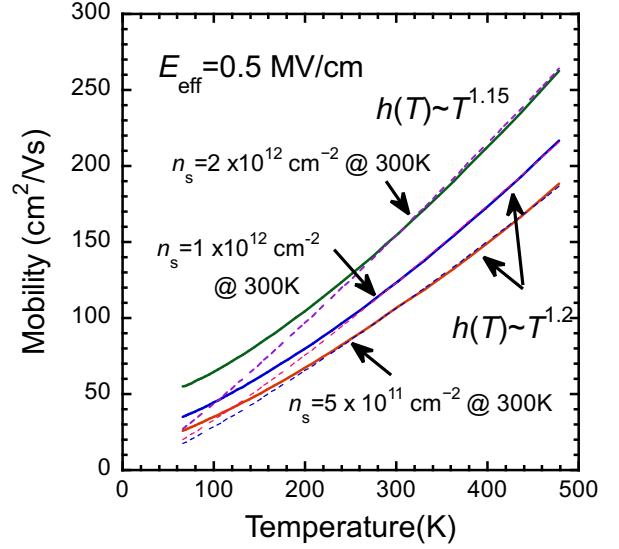


Fig. 3. Temperature dependence of dipole scattering-limited mobility for various screening conditions ( $n_s/T = \text{const.}$ ), with the effective electric field fixed at  $E_{\text{eff}} = 0.5 \text{ MV/cm}$ .

where

$$f(E_{\text{eff}}) = (E_{\text{eff}}/E_0)^{-\gamma}, \quad (10)$$

$$g_t(n_s, T) = \mu_0 \left(1 + \frac{n_s}{n_{s0}} \frac{T_0}{T}\right) \left(\frac{n_{\text{if0}}}{n_{\text{if}}}\right), \quad (11)$$

$$h(T) = \left(\frac{T}{T_0}\right)^\kappa. \quad (12)$$

The model parameters are summarized in Table II.

TABLE II  
MODEL PARAMETERS FOR CLOSED-FORM EXPRESSION OF COULOMB SCATTERING-LIMITED MOBILITY

Symbol	Value	Unit	Remarks
$\gamma$	0.55	1	exponent
$E_0$	0.33	MV/cm	normalization factor
$\mu_0$	124.57	$\text{cm}^2/\text{V}\cdot\text{s}$	
$n_{s0}$	$7.15 \times 10^{11}$	$\text{cm}^{-2}$	
$n_{\text{if0}}$	$1 \times 10^{13}$	$\text{cm}^{-2}$	normalization factor
$n_{\text{if}}$	$1 \times 10^{13}$	$\text{cm}^{-2}$	fitting parameter
$T_0$	300	K	Room temperature
$\kappa$	1.5	1	exponent

Figure 4 illustrates the procedure used to extract the temperature-dependent component of mobility under conditions of constant screening and constant effective electric field. Similar to the dipole scattering case, the mobility exhibits a power-law dependence on temperature. However, the temperature exponent  $\kappa$  for Coulomb scattering is significantly larger, with  $\kappa = 1.5$  compared to  $\kappa = 1.2$  for dipole scattering. This difference arises from the stronger energy dependence of Coulomb scattering, which leads to a more pronounced variation in the momentum relaxation time with carrier energy, and consequently, a steeper temperature dependence of the mobility.

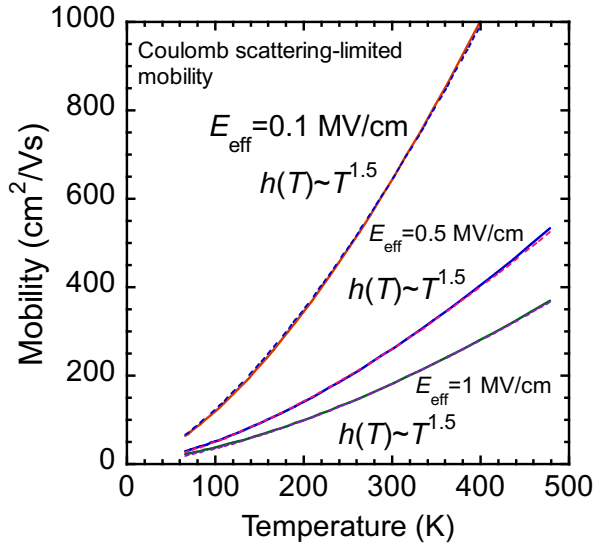


Fig. 4. Temperature dependence of Coulomb scattering-limited mobility under the constant screening condition ( $n_s/T = \text{const.}$ ), which corresponds to  $n_s = 1 \times 10^{12} \text{ cm}^{-2}$  at 300 K, for various effective electric fields  $E_{\text{eff}}$ .

### III. DISCUSSION

The theoretical analysis suggests that, under constant effective electric field and screening conditions, the temperature dependence of Coulomb scattering-limited mobility is stronger than that of dipole scattering-limited mobility. However, in practical device operation and experimental settings, it is more feasible and relevant to compare mobilities under constant gate bias, i.e., fixed sheet carrier density ( $n_s$ ).

Under constant  $n_s$ , increasing temperature weakens the screening effect, which enhances scattering and reduces mobility. Conversely, both Coulomb and dipole scattering rates tend to decrease with increasing temperature due to the increase in mean carrier energy, leading to an increase in mobility. Therefore, the observed temperature dependence of mobility arises from the competition between these opposing effects.

Figure 5 compares the calculated Coulomb and dipole scattering-limited mobilities as a function of temperature at fixed  $n_s$  and  $E_{\text{eff}}$ . The results show nearly identical temperature dependence, approximately proportional to  $T$ , indicating that the dominant scattering mechanism cannot be distinguished based solely on temperature dependence under these conditions.

This suggests that mobility measurements as a function of temperature are of limited utility in identifying the dominant scattering mechanism in SiC MOSFETs. Instead, to experimentally characterize inversion-layer mobility and deduce the scattering mechanism from its temperature dependence, measurements must be performed under the conditions developed in this study—specifically, at fixed  $n_s/T$  ratio and  $E_{\text{eff}}$ . These conditions can be experimentally realized by adjusting the gate and substrate voltages in coordination as temperature varies.

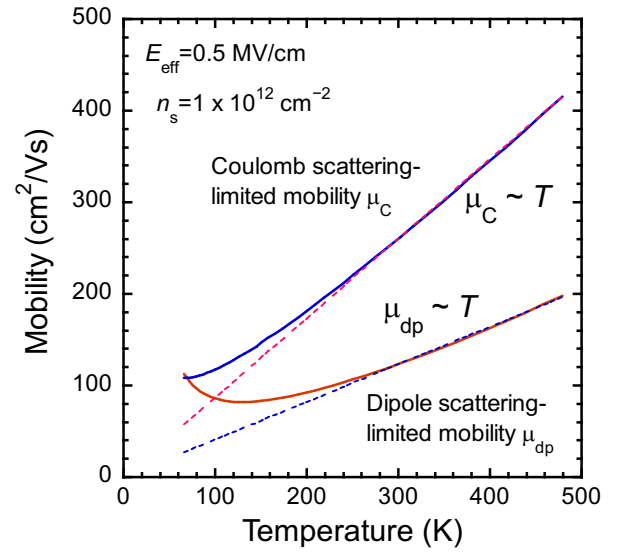


Fig. 5. Calculated temperature dependence of Coulomb and dipole scattering-limited mobilities under constant sheet carrier density ( $n_s$ ) and constant effective electric field ( $E_{\text{eff}}$ ).

### IV. SUMMARY

To enable physics-based TCAD modeling of inversion-layer mobility in SiC MOSFETs, closed-form expressions for dipole and Coulomb scattering-limited mobilities were derived based on the scattering theory of two-dimensional electron gases. These expressions incorporate temperature dependence using power-law functions with physically meaningful parameters. The resulting models can be directly implemented in TCAD frameworks and are expected to improve the accuracy of mobility prediction and aid in identifying dominant scattering mechanisms at the SiC/SiO<sub>2</sub> interface.

### ACKNOWLEDGMENT

This work was supported by the MEXT-Program for Creation of Innovative Core Technology for Power Electronics (Grant No. JPJ009777), JSPS KAKENHI Grant No. JP23K03928, and Academic Encouragement Program by Toshiba Electronic Devices & Storage Corporation.

### REFERENCES

- [1] T. Kimoto, and H. Watanabe, "Defect engineering in SiC technology for high-voltage power devices," *Appl. Phys. Express.* 13, 120101 (2020)
- [2] Shun Matsuda, Toru Akiyama, Tetsuo Hatakeyama, Kenji Shiraishi, Takashi Nakayama, "First-principles study for orientation dependence of band alignments at the 4H-SiC/SiO<sub>2</sub> interface," *Jpn J. Appl. Phys.* 63, 02SP69 (2024)
- [3] T. Hatakeyama, Y. Kiuchi, M. Sometani, D. Okamoto, S. Harada, H. Yano, Y. Yonezawa, and H. Okumura, "Characterization of Traps at SiO<sub>2</sub>/SiC (000-1) near the Conduction Band Edge by Using Hall Effect Measurements," *Appl. Phys. Express*, Vol. 10, 046601(2017)
- [4] T. Hatakeyama, H. Hirai, M. Sometani, D. Okamoto, M. Okamoto, and S. Harada, "Dipole scattering at the interface: The origin of low mobility observed in SiC MOSFETs," *J. Appl. Phys.*, Vol. 131, 145701(2022)
- [5] T. Hatakeyama, H. Hirai, M. Sometani, D. Okamoto, M. Okamoto, and S. Harada, "Physically Based Mobility Model for SiC MOSFETs in TCAD," *International Conference on Silicon Carbide and related materials 2024*, Scientific books of abstracts, vol 8, pp793-794